An instrument for investigating high electric field phenomena at small electrode separations

R. T. Olson and J. A. Panitz
Department of Physics and Astronomy, University of New Mexico, Albuquerque, New Mexico 87131

(Received 9 October 1997; accepted for publication 2 February 1998)

An instrument with the tip positioning capability of a scanning tunneling microscope and the imaging capability of a field emission electron microscope has been developed. This instrument provides the ability to investigate the current-voltage characteristics of field emitter tips in the metal-vacuum, transition, and metal-vacuum-metal tunneling regimes. It also allows a field emitter tip to be imaged before and after these ''close approach'' measurements are made. Nonreproducible tunneling characteristics observed in the transition region have been associated with large changes in the apex of the field emitter tip. © *1998 American Institute of Physics.*
[S0034-6748(98)00505-X]

I. INTRODUCTION

The high electric fields that result when voltage is applied to a sharp metal point have been utilized to investigate numerous different physical phenomena ranging from field emission to surface diffusion.[1,2] For many of these applications the sharp, pointed electrode and the counter electrode have been separated by macroscopic distances. However, an increasing number of high electric field applications, such as microfabricated field emission displays, low voltage liquid-metal ion sources, etc., require microscopic electrode separations.[3–7]

The field emission electron microscope (FEEM) and the scanning tunneling microscope (STM) image conductive substrates and characterize adsorption phenomena by the process of vacuum tunneling.[8,9] Electron tunneling in vacuum occurs when the width of the energy barrier becomes comparable to the DeBroglie wavelength of the electron in the conductor. This can occur either by a small electrode separation (as in the STM) or by a high electric field at macroscopic electrode separations (as in the FEEM). The tunneling characteristics for each case are different and identified as metal-vacuum-metal (MVM) and metal-vacuum (MV) tunneling, respectively. As the electrode separation changes between macroscopic and subnanometer distances a ''transition'' region is traversed where the electron tunneling process is not dominated by either the electric field or the electrode separation.

This article describes an instrument that combines FEEM imaging with the tip positioning ability of a STM. The instrument is particularly suited to investigate the tunneling characteristics of field emitter tips at small electrode separation distances since tips can be imaged by the FEEM before and after traversing the transition region. Previously reported experimental work in these regions is incomplete and has proven difficult to produce repeatable results.[10,11]

II. EXPERIMENTAL APPARATUS

Positioning of a field emitter tip (typically made of tungsten) is achieved using a Burleigh Aris-10 approach module.[12] The approach module is rigidly held in an OFHC copper housing that is supported by three stainless steel springs as shown in Fig. 1. The Aris-10 is capable of both coarse position control with a piezoelectric ''inchworm'' and fine position control using a quartered piezoelectric scan tube with z-axis motion of 39 Å/V.[13] For these experiments only z-axis motion is implemented.

A Macor® insulator in the top of the copper housing electrically isolates a pyrex plate coated with tin-oxide. A linear motion, ultrahigh vacuum (UHV) feedthrough provides a method of aligning the field emitter tip with either the tin-oxide coated surface or a hole (6.3 mm in diameter) in the pyrex plate. Positioning the tin-oxide surface above the tip allows it to be used as the counter electrode (anode) for ''close approach'' experiments. Alternatively, the field emitter tip can be moved through the hole so that it can be imaged on a phosphor screen (see Fig. 1). Prior to sealing the vacuum chamber, the magnification ($\sim 10^5$) of the FEEM image is chosen by moving the phosphor screen relative to the field emitter tip.

A thermionic electron gun is used to heat, and thereby clean via thermal desorption, a field emitter positioned for FEEM imaging. The electron gun is positioned ~ 3 cm from the tip such that the electron beam intersects the tip immediately above the pyrex plate. Electron energies of 3–4 keV with a total emission current of 5–10 mA heat the tip to ~ 1300 °C as judged by its yellow-white color.[14]

Several precautions have been taken to reduce the possibility of tip damage due to vibration during a close approach measurement: (1) Three beryllium copper clips hold the Macor insulator and pyrex plate rigidly with respect to the copper housing. This reduces the possibility of relative motion between the field emitter and the anode assembly. (2) The copper housing is suspended from three stainless steel springs to decouple its motion from mechanical vibrations introduced to the system. (3) Eddy current damping, supplied by three sets of rare earth magnets, critically damps any motion of the copper housing. (4) The instrument is mounted inside an ion-pumped UHV system that rests on a pneumati-

 © 1998 American Institute of Physics

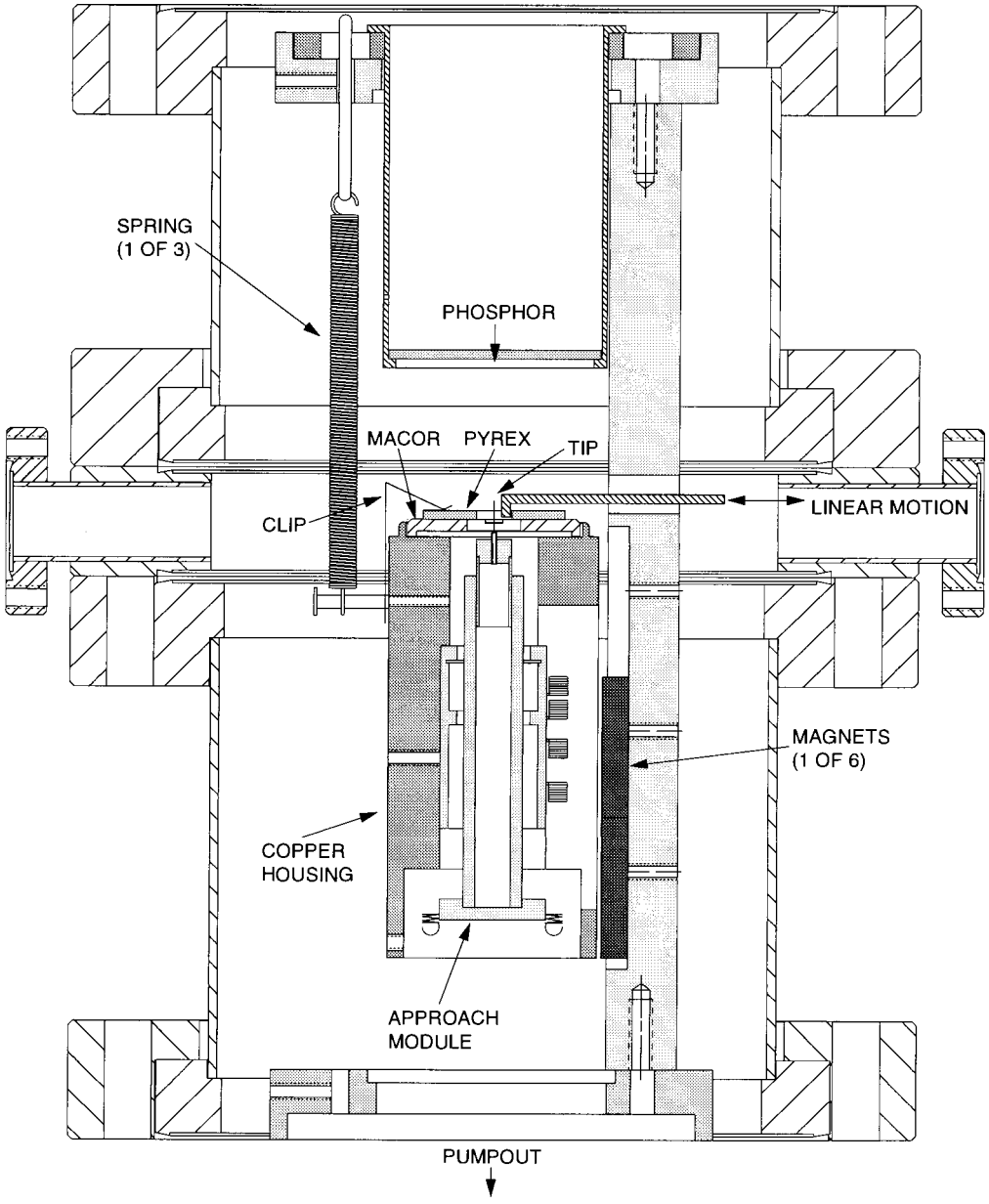

FIG. 1. A cross-sectional view of the apparatus.

cally isolated optical table. Rough pumping of the UHV system is performed with an oil-free turbo molecular pump that is disconnected from the vacuum system once the ion pump is operating. Typically experiments are performed in an UHV environment of $<=10^{-9}$ Torr that is achieved after heating the vacuum system to approximately 130 °C for 36–48 h.

A schematic of the tip positioning and data collection electronics is shown in Fig. 2. The extension element of the piezoelectric inchworm is operated by a computer-controlled 0–10 V, 16 bit digital-to-analog converter (DAC) that drives the analog input of a 0–1000 V power supply.[15,16] This allows the field emitter tip to be moved macroscopic distances with large, fixed step sizes of the inchworm (typically 3000–7000 Å/step) and also to be positioned with nanometer resolution by incrementally changing the voltage applied to the extension element. Subnanometer positioning is performed by applying voltage to the scan tube with an additional channel of the 16 bit DAC. Computer control is achieved with a LabVIEW® program that allows for either manual or automatic positioning of the field emitter tip. Automated operation adjusts the tip position by creating a linear voltage ramp with the DAC. Both the applied tip voltage and tunneling current are measured at each step of the ramping procedure

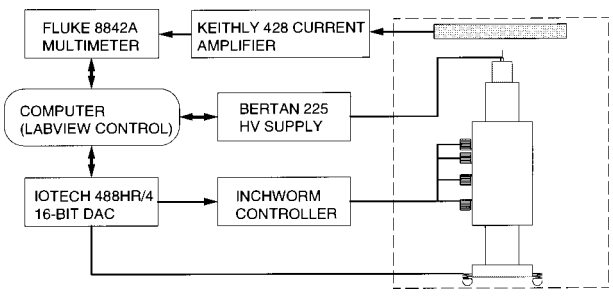

FIG. 2. Schematic of tip positioning and data collection electronics.

and the voltage ramp is terminated when the tunneling current reaches a preselected value (typically ~ 50 pA).[17]

III. *M-V* TUNNELING AND FOWLER–NORDHEIM BEHAVIOR

Fowler and Nordheim demonstrated in 1928 that electron emission from cold metals can occur via tunneling through a potential barrier modified by the presence of a high electric field (on the order of a few MV/cm).[18] The ''Fowler–Nordheim equation'' gives the electron emission current density, J (A/cm^2), as a function of electric field, F, due to this tunneling process,

$$J = c_1 F^2 \exp\left(-c_2 \frac{\varphi^{3/2}}{F}\right), \tag{1}$$

where c_1 and c_2 are constants and ϕ is the work function. A good approximation of the electric field at the surface of a field emitter tip is given by the expression $F = V/KR$, where V is the applied voltage and K is a constant (typically ~ 5), geometrical correction factor that accounts for the electrode geometry, and R is the radius of curvature of the tip apex. Substituting this expression for the electric field in the Fowler–Nordheim equation and noting that $J = I/A$, where I is the total current and A is the emitting area of the tip, results in the following linearized form,[1,8]

$$\ln\left(\frac{I}{V^2}\right) = -c_3 KR\varphi^{3/2}\left(\frac{1}{V}\right) + c_4, \tag{2}$$

where c_3 and c_4 are constants. A linear plot of current-voltage data on a graph of $\ln(I/V^2)$ vs $1/V$ identifies the MV tunneling process and distinguishes it from other tunneling phenomena. The slope of this ''Fowler–Nordheim plot'' depends only on ϕ and KR and the y intercept, c_4, is related to the emitting area at the apex of the field emitter tip.

As the anode-cathode separation distance, x, is decreased a simple calculation illustrates how the MV tunneling process occurs at lower field emitter voltages. The electric field at the tip apex is more accurately expressed by using an equation for the geometrical correction factor that describes the shape of the field emitter surface as a paraboloid of revolution.[8,19]

$$F = \frac{V}{KR} = \frac{V}{\left[\frac{1}{2}\ln\left(\frac{x}{R}\right)\right]R}. \tag{3}$$

From this equation the operating voltage of a field emitter can be predicted from the change in anode-cathode separation distance, where the subscripts i and f refer to the initial and final values, respectively.

$$V_f = V_i \frac{\ln\left(\frac{x_f}{R}\right)}{\ln\left(\frac{x_i}{R}\right)}. \tag{4}$$

For example, assume that a field emitter with a tip radius of 80 nm initially emitted a current of 1 nA at 1800 V. Reducing the electrode separation by a factor of 10^4 (i.e., $x_i = 1.0$ cm and $x_f = 1.0$ μm) would result in the same observed current at an applied voltage of only 390 V.

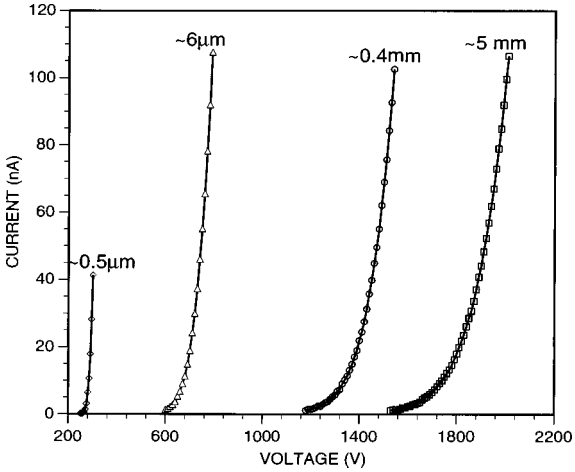

FIG. 3. Series of current voltages measurements with the electrode separation distance decreasing from approximately 5 mm to 1 μm.

Figure 3 shows the measured current-voltage characteristics for a field emitter tip operating at four distinctly different anode-cathode separation distances. The electrode separation estimated from this data decreases from approximately 5 mm down to ~ 1 μm. Figure 4 shows the same data in the form of Eq. (2) and the linear nature of the plots verifies that the measured current is due to the process of MV tunneling.

It is interesting to note that although data collected at ~ 1 μm separation exhibits typical Fowler–Nordheim behavior, the emission characteristics of the tip changed dramatically compared to the data acquired at larger electrode separation distances. This type of rapid change in both the slope and intercept of Fowler–Nordheim plots has been observed over repeated close approach measurements with numerous different field emitters.

IV. THE TRANSITION REGION

Field emitter tip positioning in the transition region is achieved by changing the electrode separation distance using the piezoelectric scan tube. Initially the separation distance is decreased with only a small potential difference between the

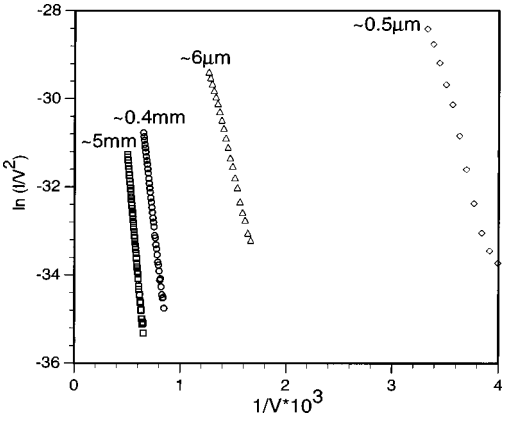

FIG. 4. The data shown in Fig. 3 plotted as $\ln(I/V^2)$ vs $1/V$.

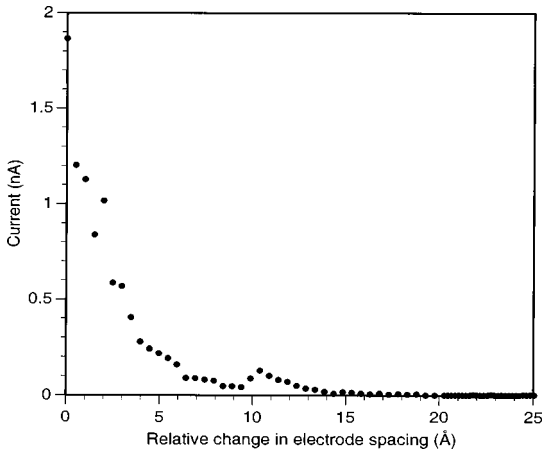

FIG. 5. With -0.1 V applied to the tip the measured current rapidly changes as the electrode spacing is decreased.

electrodes (typically 100 mV) until a current of 50 PA is measured. Since the MVM tunneling current is exponentially dependent upon the electrode spacing and linearly dependent on the voltage (for small values of V),[20,21]

$$J = c_1 V \exp(-c_2 x \overline{\varphi}^{1/2}), \tag{5}$$

where c_1 and c_2 are constants and $\overline{\varphi}$ is the barrier height above the Fermi level, the tip can be positioned within a nanometer of the anode. The tunneling current (at fixed potential difference) is then monitored as the electrode spacing is slowly increased until the current quickly drops to zero. Figure 5 shows a typical plot of current versus electrode separation that are in direct agreement with similar measurements made by Teague.[11] This technique allows a field emitter tip to be positioned within the transition region so that the tunneling behavior can be investigated.

Equation (5) indicates that the current-voltage behavior for MVM tunneling is linear, and as previously discussed, the current-voltage behavior at ''large'' electrode spacings is determined by the Fowler–Nordheim equation. The data shown in Fig. 6 was acquired with a field emitter located in the transition region. This is verified by the nonlinear current-voltage plot and nonlinear Fowler–Nordheim characteristic. It should also be noted that this result is similar to those reported by both Young and Teague.[10,11]

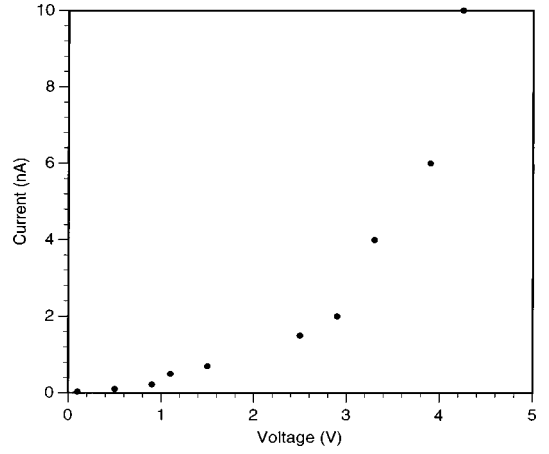

FIG. 6. Current-voltage measurement in the transition region.

Repeated attempts to acquire a complete series of current-voltage measurements as the electrode separation traversed the transition region have been unsuccessful. The primary difficulty is caused by nonreproducable tunneling current behavior as the voltage difference between the electrodes is increased. Teague has reported similar observations and noted that some improvement resulted after capacitive discharge ''cleaning'' the electrodes.[11]

V. FEEM IMAGING

Since electron tunneling behavior is dependent upon the potential energy barrier, the observed changes in Fowler–Nordheim behavior and current-voltage characteristics in the transition region must be caused by changes to the barrier. A rapid variation in electrode separation distance due to unexpected changes in the applied piezoelectric voltage, mechanical vibration, etc. could explain unpredictable current measurements in the transition region. However, this cannot explain the observed variation in Fowler–Nordheim behavior since MV tunneling current at ''large'' electrode separations is relatively insensitive to these ''small'' changes in electrode separation distance. Therefore, it is most likely that the observed tunneling behavior is caused by changes that increase the local electric field strength or decrease the work function of the field emitter surface. The ability of the instrument described here to operate as a FEEM provides a convenient method for investigating this possibility.

A FEEM forms a magnified image of a field emitter surface because electrons that escape from the tip by tunneling through the energy barrier are accelerated almost radially away from the emitter by the electric field. When the diverging electrons strike a phosphor screen a macroscopic distance away from the emitter, they produce a magnified image of the emission sites at the tip apex. The FEEM operating mode of this instrument provides a method of monitoring changes to the apex of a field emitter by imaging the tip apex before and after a measurement is made.

Altered images of the field emitter apex are commonly observed following a close approach measurement. Since electron emission from a field emitter is very sensitive to changes in work function even small amounts of gas adsorbed on the tip create a visible change in the observed emission pattern. The possibility that gaseous adsorption from the vacuum environment ($<=10^{-9}$ Torr) is responsible for the changes was eliminated by repeated FEEM imaging of a tip at macroscopic electrode separation distances. This test resulted in only very small changes in the emission pattern when compared to images of tips that had been used for a close approach measurement. Therefore, we associate the change in the emission pattern to the proximity of the electrodes during a close approach measurement.

The mechanism for this change is unknown, but adsorption of contaminants released from the anode by electron stimulated desorption seems a likely candidate. Unlike the operation field emitter tips at macroscopic separation distances, the proximity of the anode during a close approach measurement would greatly enhance the probability that desorbed contaminants would readsorb to the tip apex. We

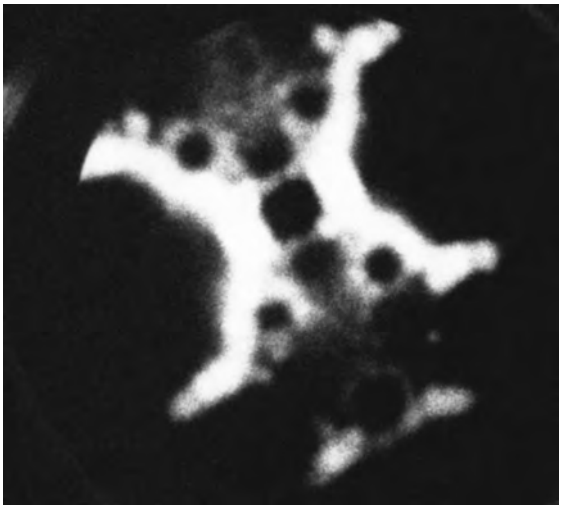

FIG. 7. Image of a tungsten field emitter tip that has been heated to ~1300 °C prior to a close approach measurement.

have observed that recleaning the field emitter after a close approach measurement commonly results in the original emission pattern as shown in Fig. 7. To eliminate the change in emission pattern in future experiments a method of providing a thoroughly cleaned, flat anode must be incorporated into the instrument. One possible method of achieving this would be to use a thin tungsten ribbon anode that could be resistively heated. Provided that the tip is protected against thermally evaporated anode material, this would result in a both a clean anode and field emitter tip prior to performing a close approach measurement.

VI. DISCUSSION

This instrument provides a method for investigating both the vacuum tunneling behavior of a field emitter at small electrode separations and changes to the emitter surface during the course of the measurements. The acquired current-voltage tunneling data and the problems encountered in data acquisition are similar to those reported by other investigators.[10,11] However, FEEM imaging before and after close approach measurements has provided insight into the difficulty of obtaining a complete set of transition region current-voltage measurements. An instrument modification that provides a clean anode surface should eliminate the problem of field emitter contamination at small electrode separation distances in future experiments.

ACKNOWLEDGMENTS

This work was supported in part by SRI International. The authors would like to thank Paul Schwoebel for many helpful discussions. The authors would also like to thank John DeMoss, Carl Allen, and John Behrendt of the machine shop and electronics shop in the Physics and Astronomy Department at the University of New Mexico. Their technical expertise was invaluable during the construction of the instrument.

[1] R. Gomer, *Field Emission and Field Ionization* (American Institute of Physics, New York, 1993).
[2] E. W. Muller and T. T. Tsong, *Field Ion Microscopy* (Elsevier, Amsterdam, 1969).
[3] C. E. Holland *et al.*, IEEE Trans. Electron Devices **38**, 2368 (1991).
[4] A. E. Bell *et al.*, J. Vac. Sci. Technol. B **6**, 306 (1988).
[5] W. Stocker *et al.*, Ultramicroscopy **31**, 379 (1989).
[6] O. Nishikawa *et al.*, J. Vac. Sci. Technol. B **14**, 2110 (1996).
[7] J. C. H. Spence *et al.*, J. Vac. Sci. Technol. B **14**, 1587 (1996).
[8] E. W. Muller, Ergeb. Exakten Naturwiss. **27**, 290 (1953).
[9] G. Binnig *et al.*, Phys. Rev. Lett. **49**, 57 (1982).
[10] R. Young, J. Ward, and F. Scire, Rev. Sci. Instrum. **43**, 999 (1972).
[11] E. C. Teague, J. Res. Natl. Bur. Stand. **91**, 171 (1986).
[12] Burleigh Instruments Inc., Aris 10 Approach Module, Fishers, NY 14453-0755 (1994).
[13] G. Binnig and D. P. E. Smith, Rev. Sci. Instrum. **57**, 1699 (1986).
[14] C. J. Smithells, *Metals Reference Handbook* (Interscience, New York, 1949).
[15] Bertan High Voltage, PMT-10C-P-3, Hicksville, NY 11801.
[16] Iotech Inc., DAC 488HR/4, Cleveland, OH 44146.
[17] Keithley Metrabyte, 428 Current Amplifier, Taunton, MA 02780.
[18] R. H. Fowler and L. W. Nordheim, Proc. R. Soc. London, Ser. A **119**, 173 (1928).
[19] W. P. Dyke and W. W. Dolan, *Advances in Electronics & Electron Physics* (Academic, New York, 1956), p. 89.
[20] J. G. Simmons, J. Appl. Phys. **34**, 1793 (1963).
[21] J. Frenkel, Phys. Rev. **36**, 1604 (1930).